

Gravitational waves from colliding black holes

Chris Pedersen

April 19, 2017

Abstract

pdftotext draft.pdf - — wc -w B B B B B Binnmaryyy..

1 Introduction

1.1 A Brief History

The first[1] and subsequent[2] observations of gravitational waves (GWs) came around the centenary of Einstein's theoretical prediction of their existence[3][4]. Einstein noticed that a solution to the linearised approximations of his field equations took the form of a wave equation[5], and that the source of these waves would be an asymmetric, massive, rotating system, such as a binary star system. As the amplitude of the waves was predicted to be so incredibly weak, with strain amplitudes on the order of 10^{-24} , at the time there was no hope of ever actually detecting them, and Einstein even questioned whether they were physically real at all[6]. Observations of the Hulse-Taylor pulsar (PSR 1913+16)[7] showed that the energy loss of the binary agreed perfectly with the rate predicted by gravitational wave emission, providing indirect evidence of GWs and resulting in the award of the 1993 Nobel Prize in Physics, but it was not until the construction of the Laser-Interferometric Gravitational wave Observatory (LIGO) that direct detection of gravitational waves became possible - a truly remarkable feat of science and engineering involving the most precise measurements ever made by several orders of magnitude.

Now that the existence of gravitational waves has been confirmed and their detection is possible we enter a new era of astronomy, and it is difficult to overstate the wealth of science that is now attainable in the coming decades. Gravitational waves can be used to study astrophysical phenomena that cannot be observed using electromagnetic radiation, such as binary black hole (BBH) systems where two inspiralling black holes merge into one, as well as being used in conjunction with electromagnetic observations in 'multi-messenger' astronomy where events such as supernovae and gamma ray bursts are thought to release both gravitational and electromagnetic radiation which can be studied in conjunction with one another[8][9]. In addition GWs can be used to conduct the closest tests of general relativity (GR) to date[10][11] as well as to further inform the ongoing development of quantum gravity models[12]. Currently the LIGO network consists of two detectors, one in Hanford WA (H1), one in Livingston LA (L1), however there are three detectors that will be added to the network in the coming years, with VIRGO (V1) in Italy due to come online by the end of 2017, and with LIGO India and KAGRA joining later. In addition to this, there are also proposals underway for a space-based gravitational wave observatory, the Laster Interferometric Space Antenna (LISA)[13] which would be able to explore a different frequency-range and therefore study a range of different astrophysical objects to those observed using earth-based detectors.

This project focuses on studying the merging of a binary system, known as a compact binary coalescence (CBC). This term includes the merging of binary neutron star systems and neutron star-black hole systems, but in this work we focus on the merging of BBHs, where we do not consider the internal structure of the compact binary objects unlike in the case of systems involving neutron stars. We focus on parameter estimation of BBH mergers, with a specific emphasis on inferring the

spin parameters of the component BHs in systems where the spins are misaligned, and how they can be determined through careful analysis of LIGO data.

The work is structured as follows; first we present an overview of gravitational wave theory and the LIGO detectors. We then discuss the process of parameter estimation and the mathematical and computational techniques that are used. Next we consider the case of systems with misaligned spins where relativistic precession is manifested, and consider the specific set of challenges this raises for signal analysis and parameter estimation. The astrophysical significance of studying precessing systems is also discussed. In chapter 2 we introduce the concept of 'matching' as a method for quantifying the degeneracy between different waveforms with minimal computational effort, and use these matches to identify the parts of the parameter space that would be most fruitful to explore. In chapter 3 we describe the process of software injections, where simulated signals are inserted into detector noise and then recovered using the inference methods introduced in the introduction. This gives a way of probing the detector response to a given signal. We present results from a range of software injections guided by the match findings, and attempt to analyse how effectively the current infrastructure is capable of inferring spin parameters on precessing BBHs. Finally we briefly consider the impact of the upcoming VIRGO detector on spin inference.

1.2 Gravitational waves and their sources

A complete analysis is available in Hartle[14], but here we briefly overview the fundamental theory of gravitational waves. In the general theory of relativity, gravity is a consequence of the curvature of a 4-dimensional spacetime as described by the Einstein equation (in natural units):

$$R_{\alpha\beta} - \frac{1}{2}g_{\alpha\beta}R = 8\pi T_{\alpha\beta} \quad (1)$$

where $R_{\alpha\beta}$ is the Riemannian curvature tensor, $g_{\alpha\beta}$ is the metric tensor, R is the Ricci scalar and $T_{\alpha\beta}$ is the energy-momentum tensor. This equation is essentially ten non-linear partial differential equations, where we use the Einstein summation convention to sum over all indices, and where indices run from 0 to 4 and all tensors are symmetric. Intuitively, the LHS of this equation can be thought of as the local curvature of spacetime, and the RHS quantifies the energy and momentum density. In the weak-field regime, where the curvature of spacetime is low, the metric tensor can be approximated as

$$g_{\alpha\beta}(x) = \eta_{\alpha\beta} + h_{\alpha\beta}(x). \quad (2)$$

where $\eta_{\alpha\beta}$ is the Minkowski metric and $|h_{\alpha\beta}| \ll 1$ for all components. This metric can be substituted into the Einstein equation, and expanding in $h_{\alpha\beta}$ in first order and using the Lorentz gauge, the Einstein equation becomes

$$\square h_{\alpha\beta} = 0 \quad (3)$$

where \square is the D'Alembertian operator, with the condition that

$$\partial_\beta h_\alpha^\beta - \frac{1}{2}\partial_\alpha h_\beta^\beta = 0. \quad (4)$$

The general solution to this equation is

$$h_{\alpha\beta} = \begin{pmatrix} 0 & 0 & 0 & 0 \\ 0 & a_+ & a_\times & 0 \\ 0 & a_\times & -a_+ & 0 \\ 0 & 0 & 0 & 0 \end{pmatrix} e^{i\omega(z-t)} \quad (5)$$

for a wave with frequency ω propagating in the z direction. Here the a_+ and a_\times terms represent the amplitudes of the 'plus' and 'cross' polarisations respectively. As a gravitational wave passes through an observer, spacetime is distorted along the spatial directions orthogonal to the propagation direction of the wave according to these polarisation amplitudes. A visualisation of this is

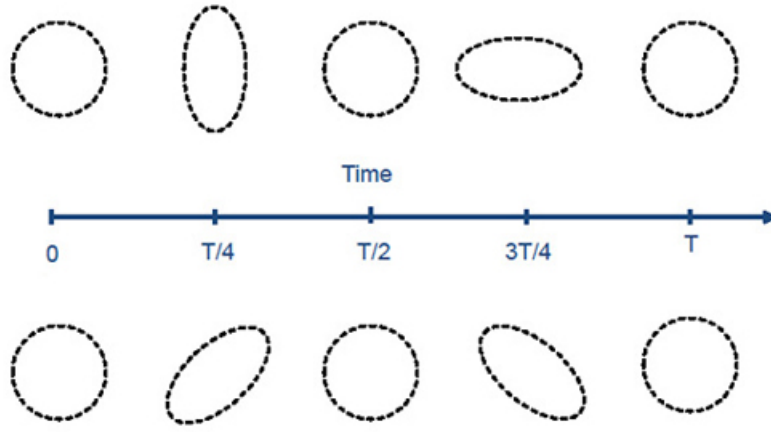


Figure 1: [15] Plus and cross polarisations respectively of a gravitational wave propagating through the page, with scale greatly exaggerated.

shown in Fig. 1. It is this stretching and squeezing of spacetime that the LIGO detectors were built to detect.

Now we consider the sources of these waves. Analysis in this area can rapidly become extremely complicated as the weak-field approximation is dropped and higher orders of perturbations are included[16], but the simplest case is still instructive.

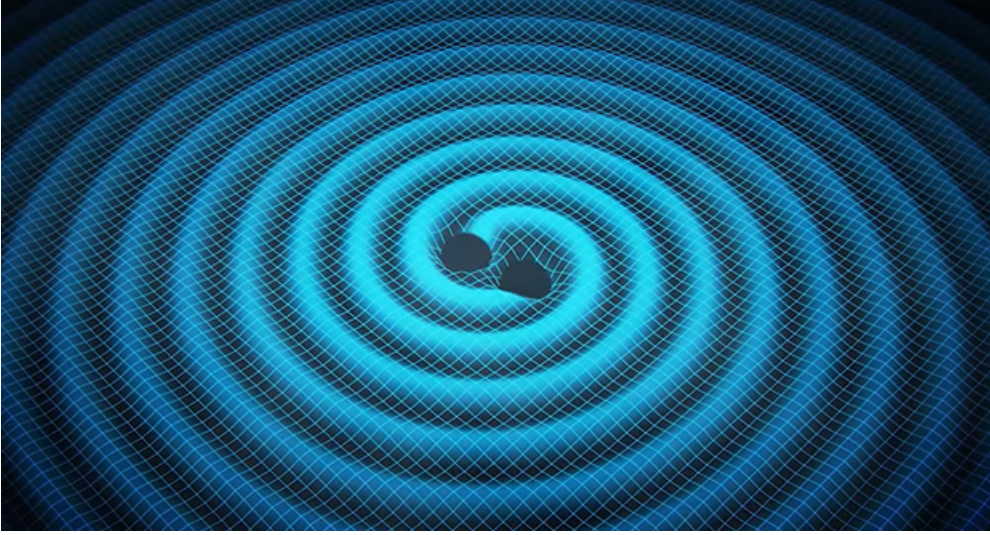


Figure 2: [17] Impression of two inspiralling compact objects emitting gravitational waves

Approximating that the field around the source is still weak, that the wavelength is long and that the observer is a large distance from the source, the spatial elements of the GW metric are

$$h_{ij} \approx \frac{2}{r} \ddot{I}^{ij}(t - r) \quad (6)$$

where I^{ij} is the second mass moment given by

$$I^{ij}(t) = \int d^3x \mu(t, \vec{x}) x^i x^j \quad (7)$$

where $\mu(t, \vec{x})$ is the mass density of the system. The energy loss of a binary system emitting gravitational waves is

$$L_{GW} = \frac{128}{5} M^2 R^4 \Omega^6, \quad (8)$$

and as the binary loses energy, the separation between the compact objects decreases, increasing the orbital frequency. Given the connection between the mass distribution of the system in (7) and the GW amplitudes in (6), this gives rise to a 'chirp' effect seen in the signal of a CBC GW. This is shown in a Fig. 3. which is a simulated waveform of the merging of a BBH system.

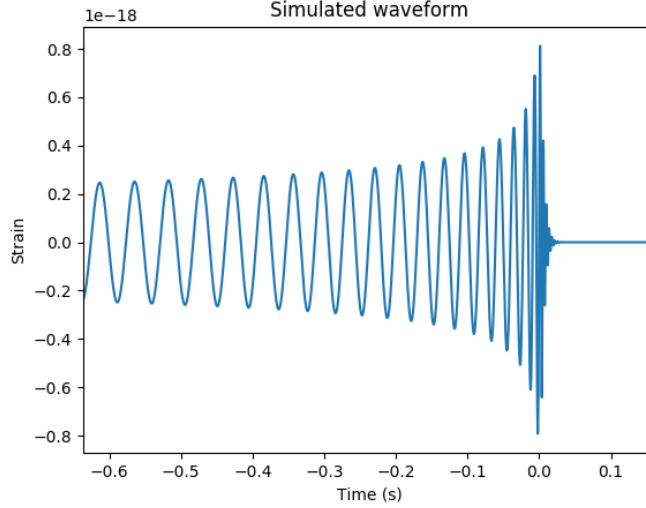


Figure 3: Simulated waveform of a BBH merger of two 35 solar mass black holes.

The waveform can be split into three phases - the inspiral, the merger and the ringdown. The frequency, frequency evolution and amplitudes of each polarisation of the GW emitted from a merger will depend on the properties of the system itself, and as such there is information about the source contained in the specific morphology of a GW signal.

1.3 LIGO

The fundamental physical principle of the LIGO detectors is that they are laser interferometers. Interferometers are devices that can measure extremely small changes in length to high accuracy using constructive and destructive interference, as shown in Fig. 4. Light leaves the laser beam, and is split down the two arms of the detector by the beam splitter. If the length of the two arms is equal, the optical path difference between the two light beams is zero, and the two beams constructively interfere after recombining at the beam splitter. However if there is any change in the length of one of the arms, the beams will no longer constructively interfere and the photodetector will register a change in intensity. As a gravitational wave passes through the detector, the relative length of the arms changes, and the GW signal is recorded by the photodiode. A large part of the scientific and engineering effort at LIGO involves techniques to minimise and account for noise in the system, and the recent advanced LIGO upgrade to the detectors increased the effective volume within which mergers can be detected by an order of magnitude[20][21]. Some of these techniques include suspending the mirrors from a series of pulleys and penduli, and applying real time corrections to the positions of the mirrors to compensate for external seismic noise. There is also considerable effort in managing the optics and lasers of the system in order to maximise the coherence of the laser beam and the intensity detected in the photodiode[22]. The noise spectrum for advanced LIGO is shown in Fig. 5.[23], where the sharp noise peaks are specifically designed

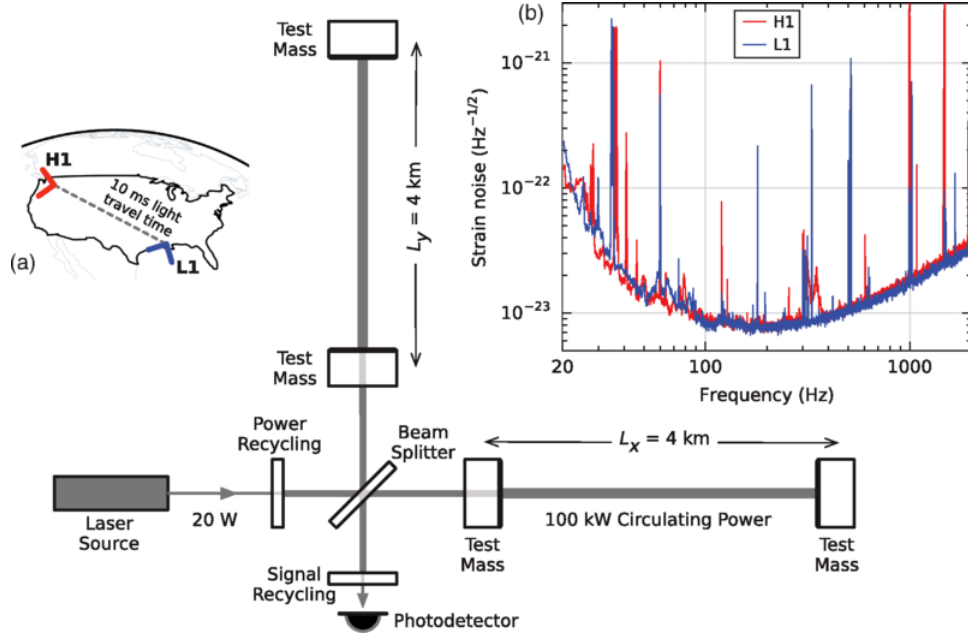


Figure 4: Simplified schematic of a LIGO detector[18] showing noise curves and detector location

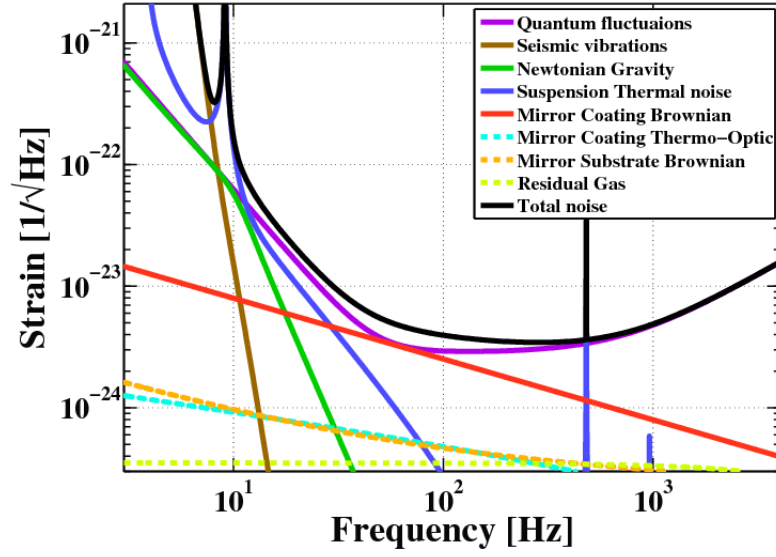


Figure 5: [19]Noise 'budget for advanced LIGO detectors.

resonances that are removed from the strain data during signal processing. The strain data observed in the detector is a function of the different polarisation amplitudes

$$h(t) = F^+(\alpha, \delta, \psi)h_+(t) + F^\times(\alpha, \delta, \psi)h_\times(t), \quad (9)$$

where $F^+(\alpha, \delta, \psi)$ and $F^\times(\alpha, \delta, \psi)$ are the antenna beam patterns that describe how the detector responds to signals at different sky locations and polarisations[24]. In first order, the polarisations are given by

$$h_+(t) = A_{GW}(t)(1 + \cos^2(\iota) \cos(\phi(t))) \quad (10)$$

$$h_\times(t) = -2A_{GW}(t) \cos(\iota) \sin(\phi(t)) \quad (11)$$

and binaries that are face on (with $\iota = 0$) emit circularly polarised waves, and edge-on binaries emit linearly (either cross or plus) polarised GWs. On completion of the advanced LIGO upgrade in 2015 the network had a detection band of 10-7000 Hz, allowing BBH mergers to be detected up to a redshift of $z=0.4$ [22]. A variety of search algorithms continuously scan the data for a variety of signals[25][26] using tailored triggers and template banks depending on the kind of search being conducted. Once a candidate signal is identified, the data around the event is then separated, and a more targeted and computationally intensive parameter estimation analysis is performed on it.

1.4 Parameter estimation

A signal is described by a total of 16 parameters[27] - time and phase of coalescence t_c and ϕ_c , two parameters to describe sky location (right ascension, α and declination δ), luminosity distance D_L , inclination angle ι describing the orientation of the binary's total angular momentum with respect to the line of sight, polarisation angle ψ , the masses m_1, m_2 , six spin parameters to totally describe the spins on each of the two black holes \vec{S}_1, \vec{S}_2 , and then two eccentricity parameters. In this work we ignore the eccentricity parameters and consider only circular orbits. The masses and spins of the component black holes are intrinsic parameters which determine the morphology of the waveform, and the remaining are extrinsic parameters. The maximum spin a black hole can have is m^2 in natural units, so the convention is to use a dimensionless spin magnitude $a = |\vec{S}|/m^2 \leq 1$. In the first order, the frequency evolution of the 'chirp' signal is approximated by a combination of the masses known as a the chirp mass

$$\mathcal{M} = \frac{(m_1 m_2)^{3/5}}{(m_1 + m_2)^{1/5}} \propto \left(f^{-11/3} \dot{f} \right)^{3/5} \quad (12)$$

so the specific morphology of the waveform is in some sense determined by a combination of the total mass and the mass ratio. We also define the total mass $M = m_1 + m_2$, and the mass ratio $q = m_2/m_1$ adopting the convention that $m_1 \geq m_2$, so $0 < q \leq 1$. Given that so many parameters, many of them extrinsic, describe only two sets of timeseries data (one from each detector), parameter estimation is a challenging task and the parameter space is both enormous and wrought with degeneracies. Two of the more thoroughly researched degeneracies are those between total mass, distance and inclination, as all three parameters scale the amplitude of the signal and between mass and spin[28], which is a degeneracy that arises out of post-Newtonian (PN) theory.

The qualitative idea behind current methods of parameter estimation is that the GW signal is processed and extracted from the raw strain data, and then matched against an array of simulated waveforms to find which waveform most closely resembles the detected signal. The two technical challenges here are quantifying how well a template represents the observed signal, and how to efficiently sample the parameter space for new templates to test against the data. A variety of methods have been employed to do this, including nested sampling[29] and analysis using Gaussian wavelets[27], and in this work we use a framework of Bayesian inference and Markov-Chain Monte Carlo methods[30][31][32]. This process results in a set of posterior distribution functions (PDFs) for each parameter. Using Bayes' Theorem, the posterior is given by

$$p(\vec{\theta}|d) = \frac{p(\vec{\theta})p(d|\vec{\theta})}{P(d)} \quad (13)$$

where $\vec{\theta}$ is an n dimensional vector in our parameter space of n parameters[29]. The first term in the numerator, $p(\vec{\theta})$ is known as the *prior* distribution, and quantifies knowledge we already have about the system that should influence our estimation of its' parameters. In practice, in inference of BBHs, the priors are almost always uniform or isotropic distributions. The denominator, $P(d)$, is essentially a normalisation factor ensuring that the posterior distribution integrates to unity. The crucial term is the *likelihood* for a given set of parameters given the data, which is determined by

$$p(d|\vec{\theta}) \propto \exp \left(-\frac{1}{2} \sum_{k=1,2} \left\langle h_k^M(\vec{\theta}) - d_k | h_k^M - d_k(\vec{\theta}) \right\rangle \right) \quad (14)$$

— signal/strain equations

Various methods of waveform generation, known as approximants, have been attempted, with varying degrees of computational intensity. In general, Post-Newtonian expansions are used in the inspiral phase where the gravitational field is weak enough for approximations to be sufficient. During the merger and ringdown, full numerical relativity simulations are required as the curvature is sufficiently strong that Post-Newtonian approximations are no longer valid[33][34].

— overview of MCMCs that will be used for inference

1.5 Precession and its astrophysical importance

Considerable research has been done on studying non-spinning binaries and on non-precessing binaries where the spins are aligned or anti-aligned with the orbital angular momentum \vec{L} [35], but it is only recently that a more complete study of the parameter space has begun[36][37]. This is partly down to computational resources, as ignoring spin effects leads to a reduced parameter space and less computationally intensive waveforms. There are a unique set of challenges when considering binaries with non-aligned spin, as due to relativistic effects, these binaries precess around the axis of total angular momentum \vec{J} , giving a time dependence to the orbital plane of the binary[38][39]. This causes the signal in the detector to have an overall amplitude modulation as a function of

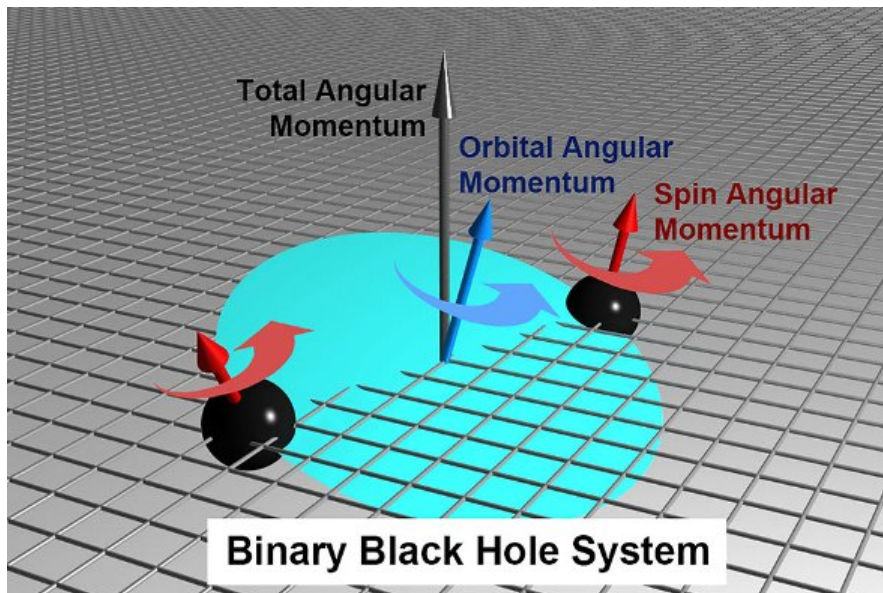


Figure 6: Illustration of a precessing binary system <https://phys.org/news/2015-03-insights-black-hole-collisions.html>

time due to the change in orientation of the source, and therefore the change in direction of peak emission of GWs. This can be seen in Fig. 7, where we compare a very slightly precessing system

with a maximally precessing one. Due to the computational intensity of dealing with both the generation of waveforms and inference process involving precessing systems, significant efforts have been made to reduce the size of the parameter space using the degeneracies between specific spin combinations to parametrise the spins of a binary. The most successful of these is the adoption of two spin parameters[34][40] that describe the whole binary system, where we replace the six spin parameters with two:

$$\chi_{\text{eff}} = \left(\frac{\mathbf{S}_1}{m_1} + \frac{\mathbf{S}_2}{m_2} \right) \cdot \frac{\hat{\mathbf{L}}}{M} \quad (15)$$

and

$$\chi_p = \frac{1}{B_1 m_1^2} \max(B_1 S_{1\perp}, B_2 S_{2\perp}) \quad (16)$$

where $B_1 = 2 + 3/(2q)$ and $B_2 = 2 + (3q)/2$. These parameters effectively quantify the amount of in-plane and out of plane spin of the total binary, removing large degenerate portions of the parameter space. As different spin configurations within these parameters are effectively degenerate, no loss of information occurs in this re-parametrisation. The recent adoption of this parametrisation in the generation of template waveform banks (the IMRPhenomPv2 waveforms which, we use in this work) has made exploring the precessing parameter space computationally viable, as it reduces the computation time by an order of magnitude. The results of these waveforms agree well with when compared with waveforms generated using the full spin parameter space (known as the Spinning Effective One Body Numerical Relativity, or SEOBNR waveforms)[41], making this an opportune time to conduct this research. Indeed the first full survey of an isotropic distribution of spins for a large number of simulations (200) has only very recently been published a matter of weeks ago[37]. The particular focus of this paper is on the challenges of inferring χ_p in precessing systems. This parameter is of particular importance due to its astrophysical implications, and as of yet there has been no comprehensive study into the effects of precession and the modulation of the signal that it involves on the process of parameter estimation. The formation methods of compact binary systems of stellar mass black holes are currently unknown, and a variety of models have been proposed[42]. Of particular interest is whether the two black holes formed from a common accreting system, or whether the binary was formed by dynamical capture. The former model would imply that the spins on the black holes would generally tend to be aligned with one another and with the orbital angular momentum, however in the dynamical capture model we expect the spins to be more or less uniformly distributed. Given the large number of expected detections over the coming years, a thorough understanding of the detector's response to precessing waveforms and an accurate estimation of our ability to recover χ_p reliably will be crucial to answering these questions, and maximising the scientific yield from this remarkable technology.

2 Precessive effects on the waveform

We first consider in closer detail the effects of precession on a GW waveform. A closer look at equation (16), which essentially quantifies the amount of precession in a given binary, shows that it takes values in the range $[0, 1]$, when the spin on the larger BH is fully in-plane. Even for a maximally precessing signal however, many possible configurations of polarisation and inclination are possible which will affect the way the amplitude of the signal is modulated. We show this in Fig. 7, where from this particular perspective the precessive effect appears largest in the case of the in-plane spin being 0.5, instead of the maximally precessing system with $|\vec{S}| = 0.98$. In this case this is due to the fact that the inclination angle is defined with respect to the total angular momentum, and so when we say we are viewing a binary 'edge-on', i.e. at $\iota = \pi/2$, the actual orbital plane of the system will not necessarily be edge-on at all for precessing systems. As a result, it is not always the case that precession affects are most noticeable in systems with the most precession, and a lot depends on the specific combination of source location and the polarisation and inclination angles for a specific event.

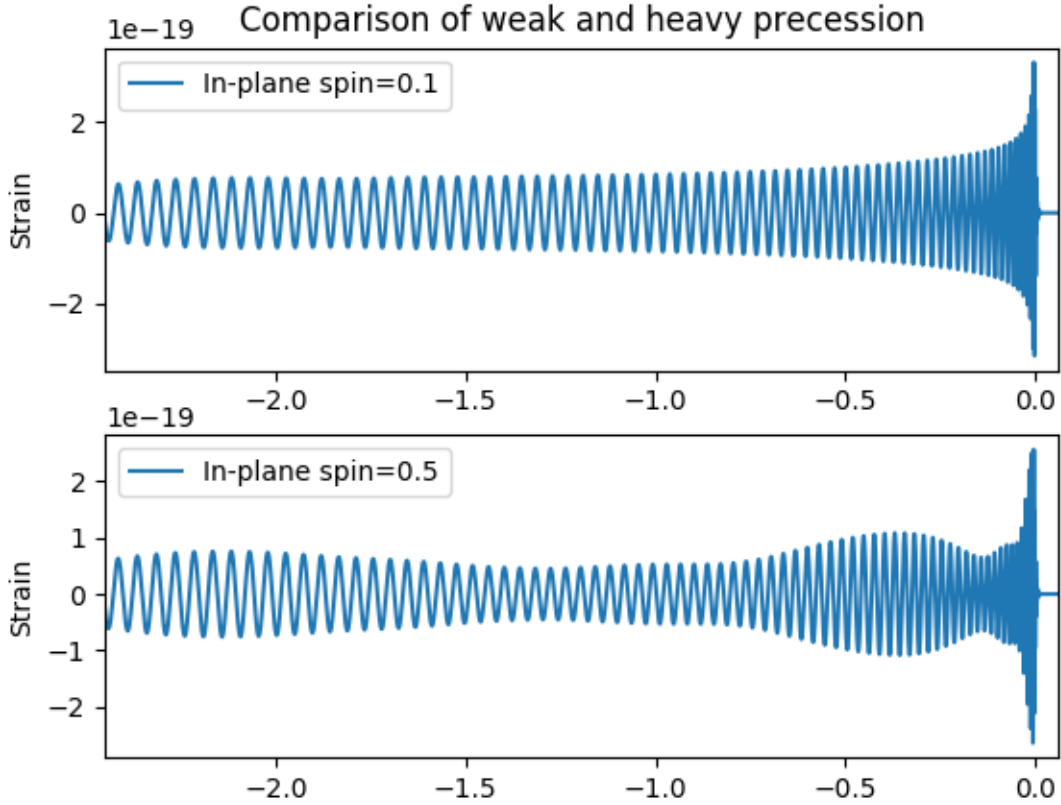


Figure 7: Waveforms for three BBH mergers with $m_1 = 30$, $m_2 = 10$ and with spins only in the x direction on the heavier black hole. The inclination is such that the binary is viewed edge-on. LEGEND ON THIS FIGURE IS WRONG, FIX BEFORE SUBMIT

3 Matching

Describe matching, and how matches are used to run targeted software injections. Then identify parameter combinations where we are particularly sensitive to χ_p , and those where we are not

4 Software injections

Describe software injections

4.1 Signal extraction

Data whitening - basically LOSC stuff, how we go from raw data to a signal - move this to intro?

4.2 Inference pipeline

Describe the structure of the inference pipeline

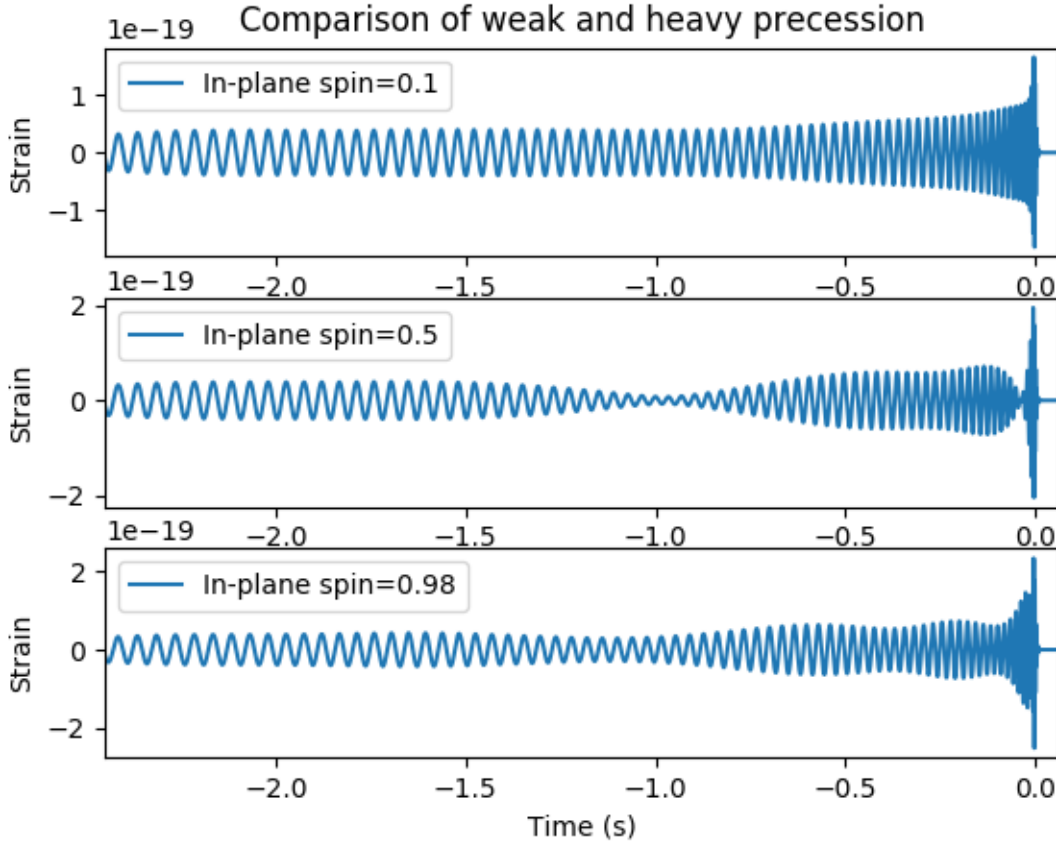


Figure 8: Waveforms for three BBH mergers with $m_1 = 30$, $m_2 = 10$ and with spins only in the x direction on the heavier black hole. The inclination is such that the binary is viewed edge-on.

4.3 Inference runs

Posteriors and discussion of inference results

4.4 Impact of Virgo

A look at how Virgo will influence PE, especially χ_p estimation

5 Conclusions and implications

Summary of results on PE and estimation of χ_p , and a prospect on Virgo's impact.

References

- [1] B.P. Abbott et. al. Observation of gravitational waves from a binary black hole merger. *Physical Review Letters*, 116(6), Feb 2016.
- [2] B.P. Abbott et. al. GW151226: Observation of gravitational waves from a 22-solar-mass binary black hole coalescence. *Physical Review Letters*, 116(24), Jun 2016.

- [3] A. Einstein. Nherungsweise integration der feldgleichungen der gravitation. *Sitzungsberichte der Kniglich Preussischen Akademie der Wissenschaften Berlin*, (688-696), 1916.
- [4] A. Einstein. ber gravitationswellen. *Sitzungsberichte der Kniglich Preussischen Akademie der Wissenschaften Berlin*, (154-167), 1918.
- [5] W. Steinicke. Einstein and the gravitational waves. *Astronomische Nachrichten*, 326(7), 2005.
- [6] N. Rosen A. Einstein. On gravitational waves. *Journal of the Franklin Institute*, 223(43-54), 1937.
- [7] J. H. Taylor and J. M. Weisberg. A new test of general relativity - gravitational radiation and the binary pulsar PSR 191316. *The Astrophysical Journal*, 253:908, Feb 1982.
- [8] Marica Branchesi. Multi-messenger astronomy: gravitational waves, neutrinos, photons, and cosmic rays. *Journal of Physics: Conference Series*, 718:022004, May 2016.
- [9] B. P. Abbott et. al. Prospects for observing and localizing gravitational-wave transients with advanced ligo and advanced virgo. *Living Reviews in Relativity*, 1:19, Dec 2016.
- [10] B. P. Abbott et al. Tests of general relativity with GW150914. *Physical Review Letters*, 116(22), May 2016.
- [11] Nicolás Yunes, Kent Yagi, and Frans Pretorius. Theoretical physics implications of the binary black-hole mergers GW150914 and GW151226. *Physical Review D*, 94(8), Oct 2016.
- [12] Xavier Calmet, Iberê Kuntz, and Sonali Mohapatra. Gravitational waves in effective quantum gravity. *The European Physical Journal C*, 76(8), Jul 2016.
- [13] Pau Amaro-Seoane et al. Low-frequency gravitational-wave science with eLISA/NGO. *Classical and Quantum Gravity*, 29(12):124016, Jun 2012.
- [14] James B. Hartle. *Gravity: An Introduction to Einstein's General Relativity*. Addison Wesley, 2003.
- [15] Unknown. Accessed 09/04/2017.
- [16] Luc Blanchet, Thibault Damour, Bala R. Iyer, Clifford M. Will, and Alan G. Wiseman. Gravitational-radiation damping of compact binary systems to second post-newtonian order. *Physical Review Letters*, 74(18):3515–3518, May 1995.
- [17] Swinburne Astronomy Productions. Accessed 09/04/2017.
- [18] Advanced ligo fig. https://upload.wikimedia.org/wikipedia/commons/d/d5/Simplified_diagram_of_an_advanced_LIGO_detector 10/04/2017.
- [19] Rana X. Adhikari. Gravitational radiation detection with laser interferometry. *Reviews of Modern Physics*, 86(1):121–151, Feb 2014.
- [20] D. V. Martynov et al. Sensitivity of the advanced LIGO detectors at the beginning of gravitational wave astronomy. *Physical Review D*, 93(11), Jun 2016.
- [21] J. et al. Abadie. Sensitivity Achieved by the LIGO and Virgo Gravitational Wave Detectors during LIGO's Sixth and Virgo's Second and Third Science Runs. 2012.
- [22] J Aasi et al. Advanced LIGO. *Classical and Quantum Gravity*, 32(7):074001, Mar 2015.
- [23] D. V. et al. Martynov. Sensitivity of the advanced ligo detectors at the beginning of gravitational wave astronomy. *Phys. Rev. D*, 93:112004, Jun 2016.

- [24] Robert L. Forward. Wideband laser-interferometer gravitational-radiation experiment. *Phys. Rev. D*, 17:379–390, Jan 1978.
- [25] C. Capano, I. Harry, S. Privitera, and A. Buonanno. Implementing a search for gravitational waves from non-precessing, spinning binary black holes. *ArXiv e-prints*, February 2016.
- [26] B. P. et al. Abbott. Gw150914: First results from the search for binary black hole coalescence with advanced ligo. *Phys. Rev. D*, 93:122003, Jun 2016.
- [27] B.P. Abbott et al. Properties of the binary black hole merger GW150914. *Physical Review Letters*, 116(24), Jun 2016.
- [28] Emily Baird, Stephen Fairhurst, Mark Hannam, and Patricia Murphy. Degeneracy between mass and spin in black-hole-binary waveforms. *Physical Review D*, 87(2), Jan 2013.
- [29] J. Veitch et al. Parameter estimation for compact binaries with ground-based gravitational-wave observations using the LALInference software library. *Physical Review D*, 91(4), Feb 2015.
- [30] M. V. van der Sluys, C. Rver, A. Stroeer, V. Raymond, I. Mandel, N. Christensen, V. Kalogera, R. Meyer, and A.M Vecchio. Gravitational-wave astronomy with inspiral signals of spinning compact-object binaries. *The Astrophysical Journal Letters*, 688(2):L61, 2008.
- [31] J. et al. Aasi. Parameter estimation for compact binary coalescence signals with the first generation gravitational-wave detector network. *Phys. Rev. D*, 88:062001, Sep 2013.
- [32] Archisman Ghosh, Walter Del Pozzo, and Parameswaran Ajith. Estimating parameters of binary black holes from gravitational-wave observations of their inspiral, merger, and ringdown. *Phys. Rev. D*, 94:104070, Nov 2016.
- [33] Alessandra Buonanno, Yanbei Chen, Yi Pan, and Michele Vallisneri. Quasiphysical family of gravity-wave templates for precessing binaries of spinning compact objects: Application to double-spin precessing binaries. *Physical Review D*, 70(10), Nov 2004.
- [34] P. Ajith, M. Hannam, S. Husa, Y. Chen, B. Brügmann, N. Dorband, D. Müller, F. Ohme, D. Pollney, C. Reisswig, L. Santamaría, and J. Seiler. Inspiral-merger-ringdown waveforms for black-hole binaries with nonprecessing spins. *Phys. Rev. Lett.*, 106:241101, Jun 2011.
- [35] Carl L. Rodriguez, Benjamin Farr, Vivien Raymond, Will M. Farr, Tyson B. Littenberg, Diego Fazi, and Vicky Kalogera. BASIC PARAMETER ESTIMATION OF BINARY NEUTRON STAR SYSTEMS BY THE ADVANCED LIGO/VIRGO NETWORK. *The Astrophysical Journal*, 784(2):119, Mar 2014.
- [36] M. V. van der Sluys, C. Rver, A. Stroeer, V. Raymond, I. Mandel, N. Christensen, V. Kalogera, R. Meyer, and A. M Vecchio. Gravitational-wave astronomy with inspiral signals of spinning compact-object binaries. *The Astrophysical Journal Letters*, 688(2):L61, 2008.
- [37] Salvatore Vitale, Ryan Lynch, Vivien Raymond, Riccardo Sturani, John Veitch, and Philip Graff. Parameter estimation for heavy binary-black holes with networks of second-generation gravitational-wave detectors. *Physical Review D*, 95(6), mar 2017.
- [38] Theocharis A. Apostolatos, Curt Cutler, Gerald J. Sussman, and Kip S. Thorne. Spin-induced orbital precession and its modulation of the gravitational waveforms from merging binaries. *Phys. Rev. D*, 49:6274–6297, Jun 1994.
- [39] Lawrence E. Kidder. Coalescing binary systems of compact objects to (post)^{5/2}-newtonian order. v. spin effects. *Phys. Rev. D*, 52:821–847, Jul 1995.

- [40] Patricia Schmidt, Frank Ohme, and Mark Hannam. Towards models of gravitational waveforms from generic binaries: II. modelling precession effects with a single effective precession parameter. *Phys. Rev. D*, 91:024043, Jan 2015.
- [41] Salvatore Vitale, Ryan Lynch, John Veitch, Vivien Raymond, and Riccardo Sturani. Measuring the spin of black holes in binary systems using gravitational waves. *Physical Review Letters*, 112(25), Jun 2014.
- [42] B. P. Abbott et al. Astrophysical implications of the binary black-hole merger gw150914. *The Astrophysical Journal Letters*, 818(2):L22, 2016.